



Dynamics and Drivers of Net Primary Production (NPP) in Southern Africa Based on Estimates from Earth Observation and Process-Based Dynamic Vegetation Modelling

26

Mulalo P. Thavhana, Thomas Hickler, Marcel Urban , Kai Heckel, and Matthew Forrest

Abstract

Terrestrial net primary production (NPP) is a fundamental Earth system variable that also underpins resource supply for all animals and fungi on Earth. We analysed recent past NPP dynamics and its drivers across southern Africa. Results from the Dynamic Global Vegetation Model (DGVM) LPJ-GUESS correspond well with estimates from the Moderate Resolution Imaging Spectroradiometer (MODIS) satellite sensor as they show similar spatial patterns, temporal trends, and inter-annual variability (IAV). This lends confidence to using LPJ-GUESS for future climate impact research in the region. Temporal trends for both datasets between 2002 and 2015 are weak and much smaller than inter-annual variability both for the region as a whole and for individual biomes. An increasing NPP trend due to CO₂ fertilisation is seen over the twentieth century in the LPJ-GUESS simulations, confirming atmospheric CO₂ as a long-term driver of NPP. Precipitation was identified as the key driver of spatial patterns and inter-annual variability. Understanding and disentangling the effects of these changing drivers on ecosystems in the coming decades will present challenges pertinent to both climate change mitigation and adaptation. Earth observation and process-

M. P. Thavhana · T. Hickler
Institute of Physical Geography, Goethe University Frankfurt am Main, Frankfurt am Main, Germany

Senckenberg Biodiversity and Climate Research Centre (SBiK-F), Frankfurt am Main, Germany
e-mail: Mulalo.Thavhana@senckenberg.de

M. Urban · K. Heckel
Department for Earth Observation, Friedrich Schiller University, Jena, Germany

M. Forrest
Senckenberg Biodiversity and Climate Research Centre (SBiK-F), Frankfurt am Main, Germany

© The Author(s) 2024

G. P. von Maltitz et al. (eds.), *Sustainability of Southern African Ecosystems under Global Change*, Ecological Studies 248,
https://doi.org/10.1007/978-3-031-10948-5_26

759

based models such as DGVMs have an important role to play in meeting these challenges.

26.1 Introduction

Plant photosynthesis on land takes up about 120 billion tons of carbon (C) per year, which is equivalent to 440 billion tons of CO₂ (Friedlingstein et al. 2020). This is about 10 times more than the global annual CO₂ emissions of 43 billion tons of CO₂ (Friedlingstein et al. 2020). About half of this uptake is used by plants as respiration to maintain their metabolism and for nutrient uptake (Gonzalez-Meler et al. 2004). The rest is available as net primary production (NPP) to grow new biomass, replace leaves and fine roots, transfer sugars to mycorrhizal fungi in the soil, and produce root exudates and biogenic volatile organic compounds (Chapin et al. 2011).

NPP is the carbon gained by plants using photosynthesis at the ecosystem level after subtracting the respiration costs, and can thus be calculated as the gross primary production (GPP) minus plant autotrophic respiration (R_a) (Chapin et al. 2011). NPP is important for providing fundamental resources for all animals and fungi on Earth including ecosystem services for people such as food, fibre, and timber production (Melillo et al. 1993; Abdi et al. 2014; Ardö 2015; Pan et al. 2015). The importance for human society can also be illustrated through the large fraction of NPP used by humans, which has been estimated as human appropriation of net primary production (HANPP) (Fetzel et al. 2012). HANPP is currently estimated to be about 25% of global NPP (Haberl et al. 2007; Niedertscheider 2011; Abdi et al. 2014; Andersen and Quinn 2020).

The main direct drivers of NPP include: temperature, precipitation, solar radiation, the CO₂ concentration in the atmosphere, nutrient availability, and vegetation structure such as the amount of leaves per ground area (Heisler-White et al. 2008; Reeves et al. 2014; Gao et al. 2016; Feng et al. 2019; Ji et al. 2020; Zhang et al. 2021). Atmospheric CO₂ influences NPP both directly as the photosynthesis of plants with the common C₃ photosynthesis partly CO₂-limited, and indirectly, as many plants reduce stomatal conductance under enhanced CO₂ levels, which can lead to more conservative water use (Archibald et al. 2009; Reeves et al. 2014; Xu et al. 2016). In savannas, these plant-physiological CO₂ effects can lead to complex changes in vegetation dynamics and fire as plants with C₄ photosynthesis, which are most savanna grasses, benefit much less from increasing CO₂ than woody plants, which can lead to woody encroachment (Midgley and Bond 2015). Terrestrial NPP patterns are expected to change in the future in response to these drivers and human population dynamics, thus necessitating assessment of NPP sensitivity to climate and other environmental change (Mohamed et al. 2004; Reeves et al. 2014). The overall vegetation NPP in warm dry regions, such as most of southern Africa is commonly mostly limited by precipitation or the amount of available moisture (Nemani et al. 2003; Hickler et al. 2005; Ji et al. 2020).

Given that NPP is one of the most variable components of the terrestrial C cycle, ecologists aim to make accurate estimates of this component when conducting research on terrestrial ecosystems, C cycles, and climate change (Sala and Austin 2000; Yu et al. 2018). Answering important questions concerning the global C balance, and predictions of the effects of global climate change rely on estimates of this fundamental quantity (Sala and Austin 2000). However, directly measuring GPP and NPP in the field is close to impossible and hence researchers resort to estimating the vegetation production components (Clark et al. 2001; Chapin et al. 2011; Peng et al. 2017).

There are various ways to estimate NPP across large extents and this includes: (1) field surveys (and subsequently extrapolating field measurements for local NPP to larger regions, using a vegetation map), (2) Earth Observation-based products, which are also informed by field survey, and (3) process-based ecophysiological modelling (Ruimy et al. 1994; Zhao et al. 2005). In this chapter, we focus on the latter two. Temporal trends, particularly if shown by both of these two approaches, will highlight whether there is increase (greening) or decrease (browning) of NPP in the study region (Zhu et al. 2016).

Southern Africa is one of the regions identified as most vulnerable to climate change (Pan et al. 2015; Ranasinghe et al. 2021; Chap. 3). Precipitation is expected to decrease over the summer rainfall region of southern Africa, and with the drying effect of increased temperature will thus lead to a robust and pronounced decrease in soil moisture over the region (IPCC 2021; Chaps. 6 and 7). In the summer rainfall areas, this is due to the El Niño/Southern Oscillation phenomenon (ENSO) which is negatively correlated with the amount of rainfall during the summer season in southern Africa (Malherbe et al. 2015; Chap. 6). Furthermore, there is high confidence in projected mean precipitation decreases in west southern Africa and medium confidence in east southern Africa by the end of the twenty-first century (Ranasinghe et al. 2021; Chap. 7).

Climate change will challenge agriculture, forestry, water systems, health, and the adaptive capacity of the natural ecosystems of the region (Pan et al. 2015). Robust projections of NPP will be highly relevant to meeting these coming challenges. However, in order to produce such projections, a solid understanding of the current NPP dynamics and drivers must be established. To this end, we seek to shed light on the following research questions: (1) what are the current NPP spatial distribution and temporal trends in southern Africa? (2) how consistent are the estimates of NPP from different methods? (3) what are the drivers of the dynamics that are producing these spatial patterns and temporal trends? and (4) can process-based models give robust estimates of future NPP by capturing these dynamics? Therefore, in this chapter, we: (1) examine and compare spatial and temporal NPP patterns for southern Africa derived from a Dynamic Global Vegetation Model (DGVM) and Earth observation-based estimates and (2) investigate some possible drivers (climate variables and atmospheric CO₂ concentration) of NPP in the region. (3) Furthermore, we subset our data using a well-known biome map to determine the NPP patterns and drivers for different ecosystems.

26.2 Materials and Methods

26.2.1 Study Region

The southern African region (here defined as -35.0 S to -20.0 S and 13.5 E to 35.0 E) is located on the southernmost part of the African continent consisting of several countries, namely: Angola, Botswana, Lesotho, Malawi, Mozambique, Namibia, South Africa, Swaziland, Zambia, and Zimbabwe. Southern Africa has both low-lying coastal areas, and mountains with varied terrain, ranging from forest and grasslands to deserts. Furthermore, the region has diverse ecoregions that includes grassland, bushveld, Karoo, savanna, and shrublands (Rutherford et al. 2006; Schoeman and Monadjem 2018). The climate across southern Africa varies from arid conditions in the west to humid subtropical conditions in the north and east, while much of the central part of southern Africa is classified as semi-arid (Cooper et al. 2004; Daron 2015). Despite the wide range of climate types, agriculture is a critical sector for all of the economies of southern African countries, so the effects of climate change on NPP and the knock-on effects on agricultural productivity, ecosystem service development, and food security are highly relevant across the study region (Gornall et al. 2010).

26.2.2 Data Sources

26.2.2.1 Earth Observation Data

MODIS and other Earth observation missions are essential tools for the development and evaluation of Earth system models predicting global ecosystem changes, which are an important information source for political decision-makers (Simmons et al. 2016; Chaps. 24 and 29). The use of Earth observation data allows the monitoring of different ecosystem variables (e.g. vegetation/biomass changes, surface moisture dynamics, etc.) with high spatial resolution and short temporal intervals (Gao et al. 2013). Earth observation data from various sources has become a valuable tool for analysing vegetation productivity in combination with *in situ* NPP estimates (Zhao et al. 2005; Fukano et al. 2021). A variety of light use efficiency (LUE) models have been developed (Running et al. 2004; Zhang et al. 2015) to calculate GPP from measured absorbed photosynthetically active radiation (APAR) (Xiao et al. 2019). Earth observation data have also been integrated with machine learning approaches (Xiao et al. 2008; Jung et al. 2009) and process-based models (Hazarika et al. 2005; Liu et al. 2019) for quantifying C fluxes (e.g. GPP and NPP). Autotrophic respiration can be estimated using modelling approaches that use daily climate variables and estimated biomass, and this can then be subtracted from GPP to derive NPP (Clark et al. 2001; Ardö 2015). In addition to estimates of these fluxes, the so-called vegetation indices (formed by combining two or more spectral bands) have been developed to characterise different aspects of vegetation from Earth observation data (Masoudi et al. 2018). Studies have shown the normalised difference vegetation

index (NDVI) to be a good proxy for NPP at high spatial resolution (Zhao et al. 2005; Pachavo and Murwira 2014; Cui et al. 2016). NDVI is expressed as:

$$\text{NDVI} = \frac{(\text{NIR} - \text{RED})}{(\text{NIR} + \text{RED})} \quad (26.1)$$

where *NIR* and *RED* are reflectance values in the near-infrared and red wavelengths, respectively (Tucker 1979). NDVI values range from +1.0 to -1.0, where negative values may be representative of cloudy conditions or areas over water bodies. Areas of barren rock, sand, or snow show very low NDVI values of 0.1–0; sparse vegetation such as shrubs and grasslands or senescing crops may show moderate NDVI values of 0.2–0.5; and high NDVI values of 0.6–0.9 correspond to dense vegetation found in temperate and tropical forests or crops at their peak growth stage (Higginbottom and Symeonakis 2014).

26.2.2.1.1 Earth Observation Platforms and Products

This study primarily utilised time series information from MODIS sensors onboard the satellites TERRA and AQUA (Minnett 2001; Yang et al. 2006; Cao 2020). Both platforms have sun-synchronous orbits with a revisit time of 1–2 days (Savtchenko et al. 2004). Data is acquired in 36 spectral bands with wavelengths ranging from 0.4 to 14.385 μm (Cao 2020).

For this study, NPP was taken from the MOD17A3 (UM Collection 5) annual totals. The MOD17 products are the first MODIS operational data sets to regularly monitor global vegetation productivity (Zhao et al. 2005; Yu et al. 2018). Details of the MODIS NPP derivations are provided in the section below.

NDVI estimates were taken from the MOD13C2 Collection 6, 16-day product (at monthly intervals) which is at 1 km spatial resolution and is provided in 0.05 degree geographic climate modelling tiles (Solano et al. 2010). The 16-day product was processed to mean annual values in R. This dataset has been used for modelling global biogeochemical and hydrologic processes in both global and regional climates (Didan 2015). Furthermore, the data have been utilised in studies to characterise land surface biophysical properties and processes, including primary production and land cover conversion (Solano et al. 2010; Didan 2015).

In addition, NDVI time series from the Advanced Very-High-Resolution Radiometer (AVHRR) sensor on board of the National Oceanic and Atmospheric Administration's (NOAA) polar-orbiting satellites was used to investigate NDVI long-term trends. Mounted on a polar-orbiting satellite it acquires images of the visible, near-infrared, and thermal infrared parts of the electromagnetic spectrum (Kidwell 1995; Sus et al. 2018). The sensor has a spatial resolution of approximately 1.1 km at satellite nadir and covers the time period from 1981 to 2015 (Trishchenko et al. 2002). NOAA AVHRR is a widely used sensor due to its long-term monitoring period and retrieval of various land surface parameters such as land cover/use dynamics, NDVI, Land Surface Temperature (LST), and Albedo (Forkel et al. 2013; Wang et al. 2020; Gulev et al. 2021; Urban et al. 2013).

26.2.2.1.2 MODIS NPP Derivation

The MOD17 algorithm is based on the original LUE logic of Monteith (1972). Input data for the model include climatic variables such as temperature, solar radiation, vapour pressure deficit (VPD) from meteorology dataset from NASA global modelling and assimilation office (Running et al. 2004). MOD15 leaf area index and fraction of absorbed photosynthetically active radiation (FAPAR) products are also utilised (Running et al. 2004; Zhao et al. 2005). Land cover classification from MODIS MCD12Q1 data product is used (Running et al. 2004). A Biome Parameter Lookup Table (BPLUT) containing values of ε_{\max} (Eq. 26.2) was derived and later updated (Running et al. 2004; Zhao et al. 2005). The table contains different vegetation types, temperature, and VPD limits and other biome-specific physiological parameters for respiration calculations (Running et al. 2004). The different vegetation types obtained from the land cover type 2 classification include: evergreen needleleaf forest, evergreen broadleaf forest, deciduous needleleaf forest, deciduous broadleaf forest, mixed forests, closed shrublands, open shrublands, woody savannas, savannas, grasslands, and croplands. Environmental multipliers represent limitations by low temperature and high VPD, and autotrophic respiration is estimated with a Q_{10} relationship (Zhao et al. 2005; Ardö 2015). The MOD17 algorithm calculates daily GPP as:

$$\text{GPP} = \varepsilon_{\max} \times 0.45 \times \text{SW}_{\text{rad}} \times \text{FPAR} \times f(\text{VPD}) \times f(T_{\min}) \quad (26.2)$$

where ε_{\max} is the maximal, biome-specific light use efficiency (g C MJ^{-1}), SW_{rad} is incoming short-wave radiation [assuming 45% to be photosynthetic active radiation (PAR)], FPAR is the fraction of photosynthetically active radiation, $f(\text{VPD})$ and $f(T_{\min})$ are linear scalars reducing GPP due to water and temperature stress (Ardö 2015). The model estimation utilises the fact that GPP is closely related to the APAR and that APAR can be measured continuously using Earth observation sensors (e.g. MODIS) (Cui et al. 2016; Xiao et al. 2019). The FPAR is estimated as a function of NDVI, derived from the standard MODIS land product (MOD15) (Eqs. 26.3 and 26.4) (Running et al. 2004; Zhao et al. 2005; Gonsamo and Chen 2017).

$$\frac{\text{APAR}}{\text{PAR}} = \text{NDVI} \quad (26.3)$$

$$\text{FPAR} = \frac{\text{APAR}}{\text{PAR}} = \text{NDVI} \quad (26.4)$$

$$\text{GPP} = \varepsilon_{\max} \times \text{PAR} \times \text{NDVI} \times f(\text{VPD}) \times f(T_{\min}) \quad (26.5)$$

$$\text{PsnNet} = \text{GPP} - R_{\text{ml}} - R_{\text{mr}} \quad (26.6)$$

NPP is calculated annually as:

$$\text{NPP} = \sum_{i=1}^{365} \text{PsnNet} - (R_{\text{mo}} + R_{\text{g}}) \quad (26.7)$$

where PsnNet is the maintenance respiration by leaves (R_{ml}) and fine roots (R_{mr}) and is calculated daily. R_{mo} is the annual maintenance respiration by all other living parts except leaves and fine roots, R_{g} is the annual growth respiration (Zhao et al. 2005).

The products were projected to a geographic grid while resampling to 0.5 degree using “average” resampling type in order to match the resolution of the climate input data used to drive our DGVM. Grid cells without valid MOD17 NPP (MOD12Q1 land cover barren, water, or urban) were masked out from the LPJ-GUESS data in order to make the data sets comparable with identical spatial extent, land cover classes, and number of grid cells. The datasets were aggregated (annual sums for NPP, annual means for NDVI) to a 14-year annual time series from 2002 to 2015.

26.2.2.2 Dynamic Vegetation Models

A class of ecosystem models known as dynamic global vegetation models (DGVMs) have been developed to simulate vegetation dynamics and biogeochemical cycling either at regional or global scales (Prentice et al. 2007; Sitch et al. 2008; Smith et al. 2014). DGVMs represent basic ecophysiological processes, such as photosynthesis, plant and soil respiration, C allocation, and plant growth, competition between plant types for resources (commonly light and water, increasingly also nutrients) and disturbances such as fire (Ardö 2015; Hantson et al. 2016). Simulating the impacts of climate change on ecosystems and feedback from ecosystems on climate, in particular via the terrestrial carbon cycle, has been a research priority (Prentice et al. 2007; Kelley et al. 2013). Subsequently, the representation of land-use has also received attention and has been integrated into DGVMs (Bondeau et al. 2007; Lindeskog et al. 2013; Pugh et al. 2019; Drüke et al. 2021).

DGVM’s largest potential lies in process-understanding (Hickler et al. 2005) rather than short-term predictions, which can be even more accurate with empirical approaches. DGVMs are powerful tools to quantify spatial and temporal variations in ecosystem C fluxes and to analyse the underlying mechanisms of NPP at large scales (Tao et al. 2003; Yu et al. 2018). DGVMs have the potential to accurately explain how ecosystem processes will interact in future climatic conditions, CO₂ concentration, nitrogen deposition, land-use changes, and soil conditions (Melillo et al. 1993; Luo et al. 2004; Ardö 2015). DGVMs are driven with climate and other environmental data (e.g. soil properties and nutrient deposition) which can be either historical (observed) data sets or projections of past/future environmental conditions.

26.2.2.2.1 LPJ-GUESS Model and Setup

The Lund–Potsdam–Jena (LPJ) model has been developed as a process-based DGVM which can efficiently represent the land–atmosphere interaction and poten-

tially be applied for broader global problems (Gerten et al. 2004; Sitch et al. 2003). The Lund–Potsdam–Jena General Ecosystem Simulator (LPJ-GUESS) framework was originally developed to add a more detailed representation of vegetation dynamics through a “forest-gap model” to the LPJ DGVM (Smith et al. 2001). Thus, LPJ-GUESS is an individual (or cohort) based model which combines biogeography and biogeochemistry typical of a DGVM with a comparatively more detailed individual and patch-based plant functional type (PFT) representation of vegetation structure, demography, growth, mortality, reproduction, carbon allocation, and resource competition (Smith 2001; Sitch et al. 2003). The model now includes an interactive nitrogen cycle (Smith et al. 2014), which can limit photosynthesis and is so important to constrain future potential CO₂ fertilisation effects (Hickler et al. 2015), and a representation of agricultural land and management (Lindeskog et al. 2013).

In the framework, productivity is simulated as the emergent outcome of growth and competition for light, space, and soil resources among woody plant individuals and a herbaceous understory in a number of replicate patches (typically 15–50) representing “random samples” of each simulated locality or grid cell (Smith 2001). Natural, cropland, and pasture land cover types are distinguished and their fractional covers are prescribed from the dataset by Hurtt et al. (2011). Within the cropland land cover type, crop fractions from the MIRCA database (Portmann et al. 2010) are used and nitrogen fertiliser application rates from Zaehle et al. (2010) are prescribed.

In this study, we used the standard version of the cohort-based LPJ-GUESS model using 20 replicate patches at a spatial resolution of $0.5^\circ \times 0.5^\circ$. Climate forcing data from the CRU JRA v2.0 dataset (details below) were used. Land-use dataset by Hurtt et al. (2011) was included. The global plant functional types (PFTs) analysed in our model were: boreal needleleaf evergreen (BNE), boreal shade-intolerant needleleaf evergreen (BINE), boreal needleleaf summergreen (BNS), temperate needleleaf evergreen (TeNE), temperate broadleaf summergreen (TeBS), shade-intolerant broadleaf summergreen (IBS), temperate broadleaf evergreen (TeBE), tropical broadleaf evergreen (TrBE), tropical shade-intolerant broadleaf evergreen (TrIBE), tropical broadleaf raingreen (TrBR), C3 grasses (C3G), C4 grasses (C4G). The model output includes GPP, NPP ($\text{kg C m}^{-2} \text{ year}^{-1}$), respiration, carbon pools, burnt area fraction, and potential vegetation among other outputs. The model was run on a daily time step. All simulations were initialised with a 500 years spinup to allow vegetation, soil carbon and nitrogen pools to build up from “bare ground” to a “steady state” and then the full transient period (1901–2018) was simulated. Fire was enabled through the SIMFIRE-BLAZE fire model (Knorr et al. 2016; Nieradzik et al. 2015).

26.2.2.3 Meteorological Data

Precipitation, temperature, and solar radiation data from the CRU JRA v2.0 dataset were used for both driving the LPJ-GUESS simulations and for investigating the correlation between NPP and its potential drivers. As a basis, this dataset starts with the Japanese reanalysis (JRA) (Harada et al. 2016; Kobayashi et al. 2015) data produced by the Japanese Meteorological Agency (JMA). This is then adjusted,

where possible, to align with the monthly values of the CRU TS 3.26 dataset (Harris and Jones 2019), a gridded land surface dataset based on meteorological station data produced by the Climatic Research Unit (CRU). The data availability spans from January 1901 to December 2017. The dataset is a 6-hourly, gridded time series of ten meteorological variables and is intended to be used to drive models of the global land surface and biosphere such as DGVMs. The variables are provided on a 0.5×0.5 degree grid.

26.2.3 Data Analysis

NDVI time series from MODIS and AVHRR products along with MODIS NPP products were used to assess the vegetation productivity. NPP was simulated to assess whether the LPJ-GUESS model agrees with MODIS and AVHRR estimates by following the inter-annual variation of remotely estimated NPP and NDVI. This was to evaluate the model's capability to reproduce past data and ultimately adopted for future predictions in southern Africa.

The potential driving factors and trend analysis of NPP and NDVI were conducted per biome, according to the South African National Biodiversity Institute (SANBI) 2006 biome map (Fig. 26.1) (Rutherford et al. 2006). The biome map is made up of nine well-established biomes in South Africa which includes: Savanna, Grassland, Nama Karoo, Succulent Karoo, Fynbos, Albany Thicket, Forest, Indian Ocean Coastal Belt (IOCB), and Desert (Rutherford et al. 2006). This was to show the ecological and climatic variability experienced across the South African region. Although the study area covers southern Africa and not just South Africa, the SANBI biome was used because it has been studied extensively. Furthermore, the

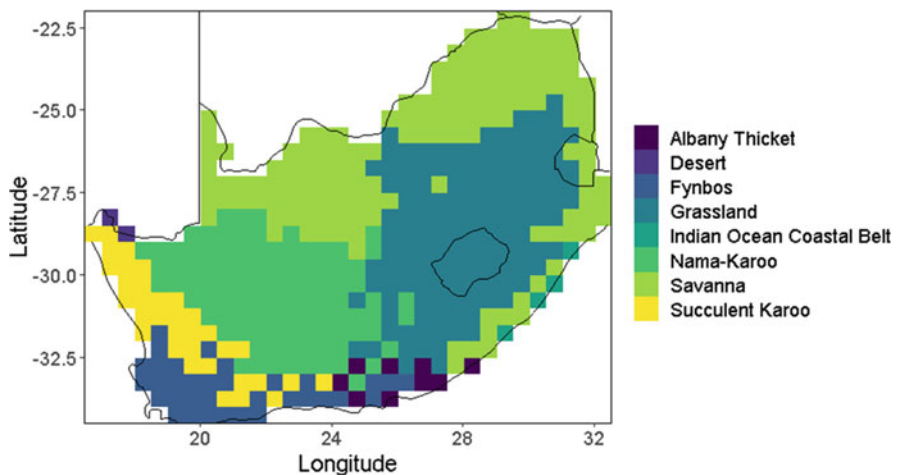


Fig. 26.1 South African National Biodiversity Institute (SANBI) 2006 biome map by Rutherford et al. (2006)

study focuses on the dynamics and drivers of NPP per biome where actually the South African biomes extend into the upper regions of the study area.

26.2.3.1 Analysis Software

The R statistical programming language was used for processing and for statistical analysis of the data. MODIS R package (Mattiuzzi et al. 2017) was used to download and process MODIS data. We used the DGVMTools R package¹ to perform comparisons, analysis, and plotting of the spatially explicit simulated and remotely sensed NPP distribution across the study region. DGVMTools is a high-level framework for processing, analysing, and visualising DGVM data output which easily interfaces with both the raster package and base R functionality. The *ggplot2* package (Wickham 2016) was used for additional plotting and linear trend analysis.

26.2.3.2 Time Series Analysis

The NDVI and NPP time series were analysed along with the key climate variables (precipitation, temperature, and solar radiation) over the period 2002–2015. The region experienced extreme rainfall events in the year 2000 which were far outside its normal variability (Dyson and van Heerden 2001; Smithers et al. 2001). Accordingly, the years 2000 and 2001 were excluded from the analysis since including them was found to produce spurious trends and thus produced misleading analysis and conclusions. The AVHRR NDVI time series were analysed from 1982 to 2015 in order to gain some perspective of the longer NDVI trend. As these variables have different units and magnitudes, we derived aggregated standardised anomalies following Seaquist et al. (2008) and this is expressed as:

$$\text{Standardised anomaly} = \frac{(x - \bar{x})}{\text{sd}} \quad (26.8)$$

where x is the annual mean values, \bar{x} is the mean of the annual mean values, and sd is the standard deviation.

Linear trends were fitted to NDVI and NPP time series to determine the productivity long-term trend (Higginbottom and Symeonakis 2014). Due to the large inter-annual variation and relatively short time series of our data, most trends are not statistically significant. The Mann-Kendall test (Mann 1945) was used to quantify the significance and only $p < 0.05$ was considered. We also analysed the response of LPJ-GUESS simulated NPP to atmospheric CO₂ concentration by comparing the standard LPJ-GUESS simulation to one with atmospheric CO₂ concentration fixed from 1901 at its corresponding value of 296.4 ppm.

¹ <https://github.com/MagicForrest/DGVMTools>

26.2.3.3 Statistical Correlation Analyses

We used Pearson's product moment correlation coefficient (r) to quantify the level of agreement between LPJ-GUESS and MODIS NPP. To examine the relationship between different variables (NPP, NDVI, CO₂, and different climate factors) Spearman's rank correlation coefficient was used. This is because we are interested in monotonic relationships between these variables which do not necessarily need to be linear. Spearman's coefficient is insensitive to any nonlinearity that could undermine the detection of a monotonic relationship between the variables. The coefficient ranges from -1 to $+1$ and was examined using the "PerformanceAnalytics" R package (Peterson et al. 2020). Large positive values indicate strong agreement, large negative values indicate strong disagreement, and values near 0 indicate random agreement (Seaquist et al. 2008; Bon-Gang 2018).

26.3 Results

26.3.1 NPP Geographical Patterns

The broad spatial patterns of NPP are as expected, with higher NPP in regions of higher rainfall and lower NPP in areas that experience extreme heat and receive less rainfall. In general, NPP simulated by LPJ-GUESS and estimated by MODIS showed similar spatial patterns, with Pearson's $r = 0.85$ and Root Mean Squared Error (RMSE = 0.1446 kg C m⁻² year⁻¹). The main difference is lower LPJ-GUESS simulated NPP values along the coastal regions (Fig. 26.2). Contrastingly, LPJ-GUESS showed higher NPP than MODIS as one moves in from the coast. The inter-annual dynamics of NPP on a gridcell level correspond reasonably well. This is indicated by Pearson's correlation coefficients of the time series of the individual

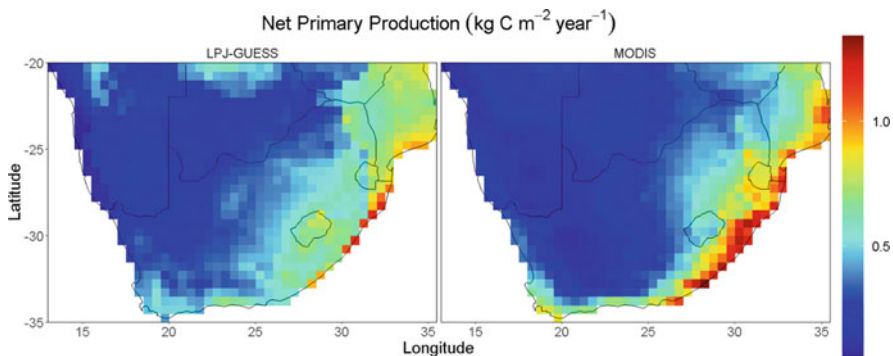


Fig. 26.2 Spatial distribution of modelled NPP and remotely sensed NPP averaged over time (2002–2015) to evaluate spatial patterns of NPP over the southern African region. The plot presents a strong linear relationship between LPJ-GUESS and MODIS of $r = 0.85$ and RMSE = 0.1446 (kg C m⁻² year⁻¹)

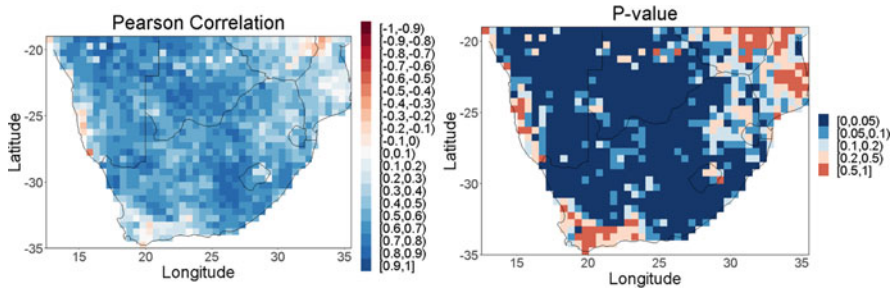


Fig. 26.3 Pearson correlation and significance level of modelled NPP and Earth observation-based NPP per gridcell, averaged over time (2002–2015). The plot presents a high correlation of LPJ-GUESS and MODIS NPP over most parts of the region with great significance level ($p < 0.05$) within the correlated areas

grid cells with high statistical significance ($p < 0.05$) over most parts of the study region (Fig. 26.3).

26.3.2 NPP Temporal Development

When averaged over the whole study region, LPJ-GUESS simulated and MODIS-estimated NPP showed good agreement in terms of the overall magnitude and inter-annual variation (Fig. 26.4). The inter-annual variation was found to be large, annual values ranged from a maximum of over $0.5 \text{ kg C m}^{-2} \text{ year}^{-1}$ in 2006, to less than $0.35 \text{ kg C m}^{-2} \text{ year}^{-1}$ (minima in 2003 and 2015). The time series also revealed a small tendency of the LPJ-GUESS model to simulate higher values than estimated with MODIS. However, when applying the Mann-Kendall test the trends showed no significance.

Considering NPP times series per biome (Fig. 26.1; Chap. 3) gives a more nuanced view of the regional disparities between LPJ-GUESS and MODIS (Fig. 26.5). The grass-dominated biomes (Grassland and Savanna) showed good agreement in NPP magnitude between LPJ-GUESS and MODIS, the tree-dominated biomes (Forest, Albany Thicket, and Indian Ocean Coastal Belt) and Fynbos showed consistently higher NPP in MODIS than LPJ-GUESS. This pattern is reversed for the most arid biomes (Nama Karoo, Succulent Karoo, and Desert) where LPJ-GUESS simulates higher NPP. Both LPJ-GUESS and MODIS NPP showed a similar increasing but weak trend for the majority of the biomes (Fig. 26.5). However, on a per grid cell basis, the majority of the region shows no significant trends for both the LPJ-GUESS and MODIS NPP (Fig. 26.6b).

Examination of simulated LPJ-GUESS NPP over a longer period (1901–2015) showed high inter-annual variation against a backdrop of increasing NPP (Fig. 26.7b) caused by rising atmospheric CO_2 (Fig. 26.7a). According to the model, NPP has increased by 18% since 1901. This is in agreement to the increasing trend for

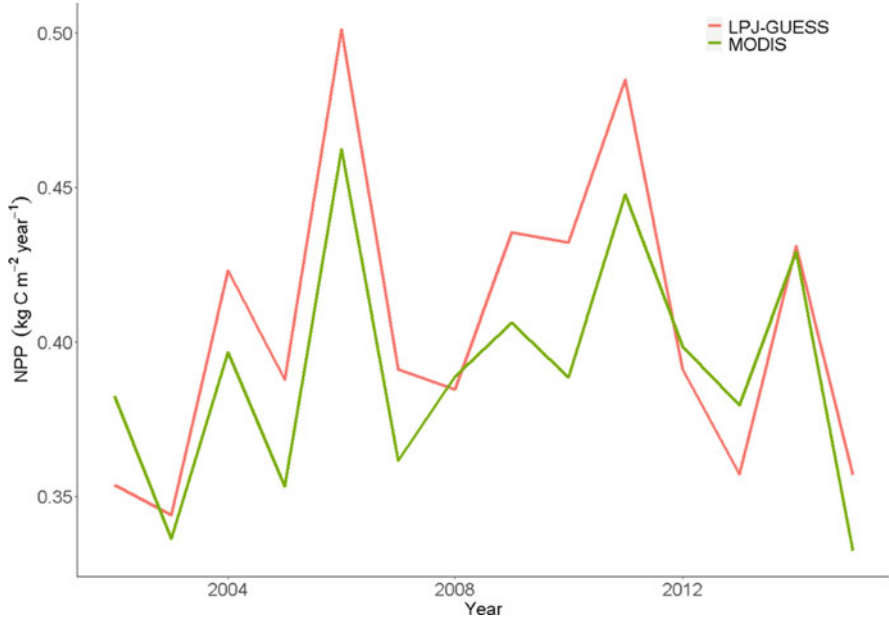


Fig. 26.4 Temporal distribution of LPJ-GUESS modelled and MODIS-estimated NPP ($\text{kg C m}^{-2} \text{ year}^{-1}$) averaged over the whole southern Africa study region



Fig. 26.5 Absolute values and linear trends of NPP ($\text{kg C m}^{-2} \text{ year}^{-1}$) and NDVI (unitless) per biome

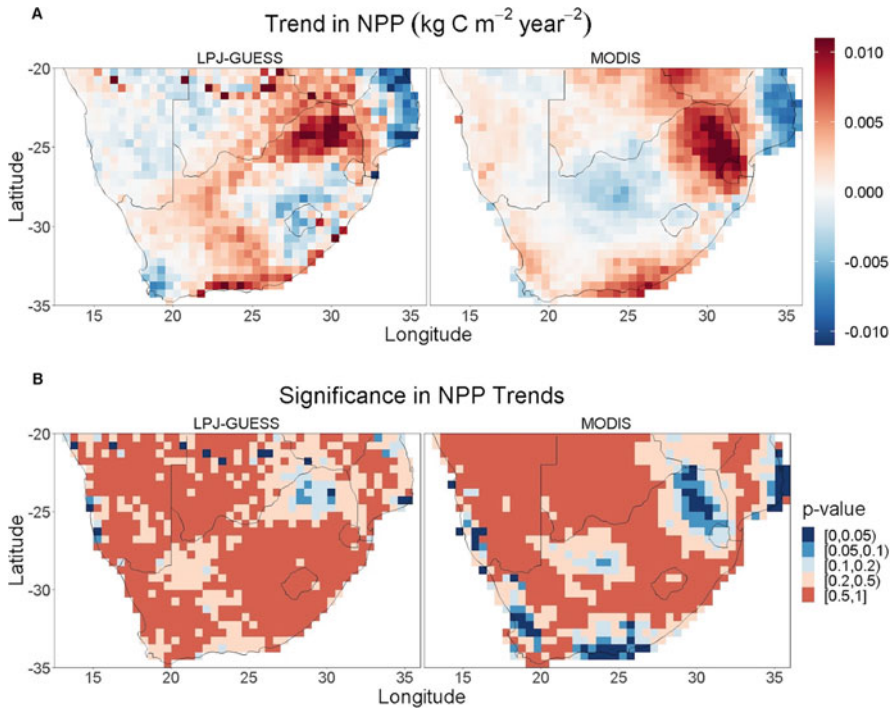


Fig. 26.6 (a) Trend in modelled and Earth observation NPP. (b) The significance in trends for both modelled and Earth observation NPP. The majority of the region shows no significant trends for both products

2002–2015 (Fig. 26.4). This longer term trend in NPP is significant (Mann-Kendall $p < 0.00005$).

The longer time series of AVHRR data averaged over the whole study area showed a strong increase in NDVI from 1982 to 2015 and a Mann-Kendall test of trend significance revealed high statistical significance with a $p < 0.0048$ (Fig. 26.7b). Comparison of NPP and NDVI showed increasing trends (Figs. 26.5 and 26.7b) for all biomes except for decreasing trends in the desert and flat trends in the IOCB for MODIS NDVI and NPP. However, the trends showed no significance for the Mann-Kendall test except for MODIS NPP in the Fynbos ($p = 0.037$) and forest ($p = 0.016$) (data not shown). The decadal scale fluctuations were apparent in the longer term time series with some periods of increasing and declining NPP, thus indicating that the increasing NPP observed for 2002–2015 is not necessarily a new phenomenon or a result of global change, but could simply be a consequence of decadal scale climate variability.

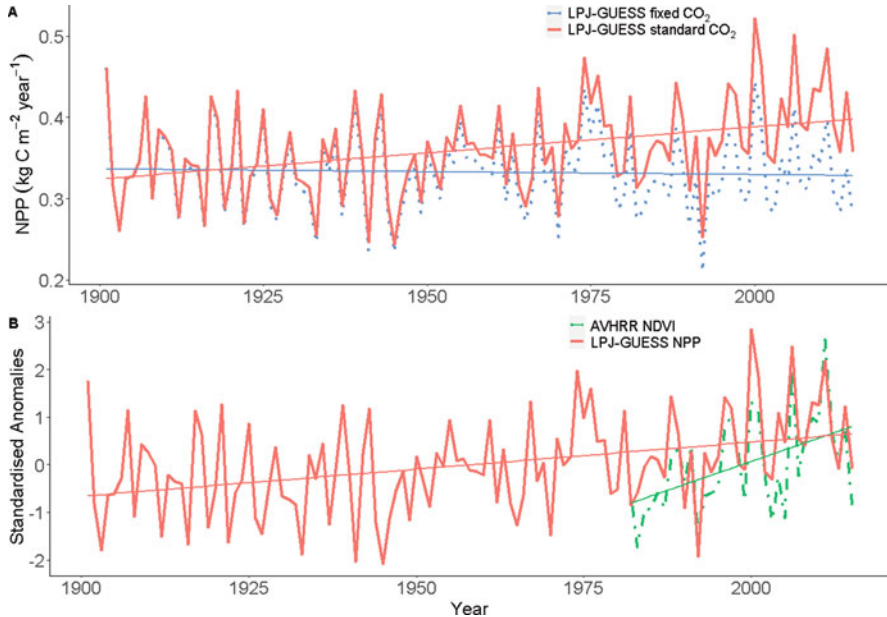


Fig. 26.7 (a) Annual average NPP ($\text{kg C m}^{-2} \text{ year}^{-1}$) across the whole study region simulated by LPJ-GUESS with historically varying atmospheric CO_2 concentration and CO_2 fixed at values from the year 1901 (296.3785 ppm) and (b) Aggregated standardised anomalies of historical LPJ-GUESS NPP (1901–2015) and AVHRR NDVI (1982–2015). This plot evaluates the trends and Inter-annual variability (IAV) of NPP over a longer time span

26.3.3 NPP and NDVI Correlations

The LPJ-GUESS and MODIS NPP showed high Pearson correlation coefficient (ranges from 0.68 to 0.82) throughout the biomes except for Fynbos (0.37) (Table 26.1). The correlations between the two products showed significance of $p < 0.001$ while Fynbos showed no significance. Succulent Karoo (0.49), Albany Thicket (0.50), and IOCB (0.16) showed no significance when comparing LPJ-GUESS NPP and MODIS NDVI while high and significant ($p < 0.001$) correlation was observed for the rest of the biomes (ranges from 0.64 to 0.91). The IOCB biome (0.36) showed low and not significant correlation when comparing MODIS NPP and NDVI, while the rest of the biomes showed significantly high correlations (ranges from 0.61 to 0.93).

26.3.4 Potential Driving Factors of NPP

Precipitation showed similar inter-annual variation to that of LPJ-GUESS and MODIS NPP per biome, as demonstrated by significantly high correlations with

Table 26.1 Spearman rank correlation coefficient for aggregated standardised anomalies (MODIS NDVI, MODIS NPP, LPJ-GUESS NPP, precipitation, temperature, and solar radiation) per biome, from 2002 to 2015. The Pearson correlation was applied for the LPJ-GUESS and MODIS NPP comparisons. The table shows the value of the correlation plus the significance level as stars. Each significance level is associated to a symbol: p -values (0, 0.001, 0.01, 0.05, 0.1, 1) refers to symbols (***, **, *, †, **) respectively

Biome	NPP_LPJ-GUESS				NPP_MODIS				NDVI_MODIS				Precipitation		Temperature	
	Precipitation		Temperature		Solar radiation		NDVI_MODIS		NPP_MODIS		Precipitation		Temperature		Solar radiation	
	Precipitation	Temperature	Solar radiation	NDVI_MODIS	NPP_MODIS	Precipitation	Temperature	Solar radiation	NDVI_MODIS	Precipitation	Temperature	Solar radiation	Temperature	Solar radiation	Temperature	Solar radiation
Desert	0.81***	-0.44	-0.31	0.82***	0.69**	0.42	-0.064	-0.48†	0.89***	0.58*	-0.20	-0.45	-0.51†	-0.10	0.42	
Succulent Karoo	0.84***	-0.39	-0.32	0.49†	0.68**	0.56*	-0.077	-0.30	0.86***	0.43	-0.033	-0.30	-0.37	0.051	0.073	
Nama Karoo	0.84***	-0.015	-0.73**	0.68**	0.81***	0.70**	-0.56*	-0.65*	0.73**	0.75**	-0.14	-0.79**	-0.13	-0.85***	0.21	
Fynbos	0.89***	-0.40	-0.27	0.64*	0.37	0.42	-0.086	0.0022	0.64*	0.56*	-0.24	0.046	-0.45	-0.059	-0.20	
Albany Thicket	0.81***	-0.27	-0.58*	0.50†	0.70**	0.70**	-0.40	-0.25	0.62*	0.55*	-0.16	0.0022	-0.40	-0.29	-0.064	
Grassland	0.92***	-0.30	-0.76**	0.91***	0.78**	0.79**	-0.50†	-0.65*	0.76**	0.86***	-0.27	-0.78**	-0.42	-0.74**	0.44	
Savanna	0.84***	-0.13	-0.61*	0.81***	0.74**	0.95***	-0.55*	-0.73**	0.93***	0.93***	-0.39	-0.81***	-0.38	-0.71**	0.35	
Forest	0.85***	-0.38	-0.37	0.70**	0.82***	0.61*	-0.22	-0.25	0.61*	0.80***	-0.17	-0.13	-0.33	-0.35	0.015	
IOCB	0.95***	-0.48†	-0.13	0.16	0.72**	0.58*	-0.67*	-0.11	0.36	0.0022	-0.35	-0.43	-0.35	-0.099	0.36	

[†]Pearson correlation

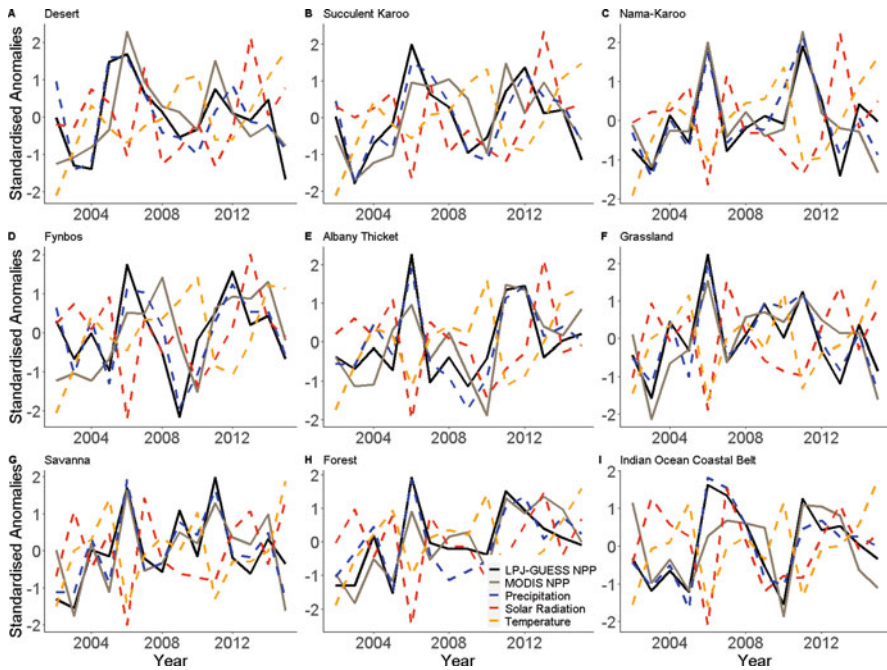


Fig. 26.8 Aggregated standardised anomalies of precipitation, temperature, and solar radiation in comparison with both the modelled and Earth observed NPP per biome

both MODIS (0.56–0.95) and LPJ-GUESS NPP (0.81–0.95) (Fig. 26.8 and Table 26.1). However, there were two notable exceptions to this: the correlations between MODIS NPP and precipitation in the Desert (0.42) and Fynbos (0.42) biomes were low and not significant. In contrast, solar radiation and temperature showed negative correlations with MODIS and LPJ-GUESS NPP across all biomes, although they were not significant in most cases (Table 26.1). Of all the climate drivers, temperature showed a significantly increasing trend with the Mann-Kendall $p < 0.049$ for Succulent Karoo and 0.009 for Desert while the rest were not significant. This is consistent with global warming in areas of high inter-annual variability and relatively short time series (as is the case here).

The model simulation in which atmospheric CO_2 concentration was held constant at 1901 levels (Fig. 26.7a) showed that increasing CO_2 concentration is responsible for a large increase in NPP. This effect was built to be around +18% ($+0.064 \text{ kg C m}^{-2} \text{ year}^{-1}$) by 2015. LPJ-GUESS NPP showed a slight decline without significant trend when the effects of increasing atmospheric CO_2 were removed.

26.4 Discussion

26.4.1 Comparison of NPP from Modelling and Earth Observation Products

The DGVM LPJ-GUESS and MODIS NPP products show similar spatial patterns, temporal trends, inter-annual variability, and good correlation (Figs. 26.2, 26.3, and 26.4). The good correspondence and correlation is encouraging as both methods are largely independent and only share some common input variables (e.g. daily precipitation and temperature), but from different data sets. The correspondence between MODIS17 and LPJ-GUESS here appears to be slightly better than in comparison with an earlier LPJ-GUESS version applied to simulate all of Africa by Ardö (2015), which did not include land-use and nitrogen limitation to vegetation growth and had a different fire module.

Both the MODIS and LPJ-GUESS estimates are to a greater or lesser extent model derived estimates and so subject to uncertainty in the parameters used, the input data and, in the case of LPJ-GUESS, uncertainty in the process representations. The MODIS estimate might be expected to be the more reliable as it uses Earth observation FPAR as an input (which means it is more constrained) (Myneni et al. 1999, 2002; Running et al. 2004), while FPAR in LPJ-GUESS emerges from complex equations that govern the growth of and competition between plant functional types (PFTs) and disturbances (Smith 2001; Sitch et al. 2003). It should also be noted that the MODIS NPP algorithm has been criticised, e.g., for its assumed temperature effects (Medlyn 2011), and the representation of environmental controls of NPP is not very sophisticated, see above. However, given that MODIS NPP uses Earth observation FPAR and so is in principle better constrained, we can interpret the comparison of LPJ-GUESS with MODIS as an evaluation of LPJ-GUESS to some extent. As we find good correspondence between the two, we can conclude that past and future projections for southern Africa are also reliable.

LPJ-GUESS is commonly used to derive future projections to guide climate adaptation and mitigation measures, so this result is promising and indicates that LPJ-GUESS can be fruitfully applied to the study area. As a small caveat, it should be noted that the per biome comparisons between MODIS and LPJ-GUESS did show some disparities in the more arid and the more tree-dominated biomes. This is not surprising as we applied the standard global LPJ-GUESS configuration here and a global model cannot be expected to reproduce all the features of a diversely vegetated region such as southern Africa. Future studies would benefit from using a regionally parameterised version of LPJ-GUESS, in particular the inclusion of shrub PFTs to better represent the arid regions.

All analysed time series products (LPJ-GUESS and MODIS NPP, and MODIS and AVHRR NDVI) show increasing trends for all the biomes except for the desert which showed a decreasing trend and grasslands which showed no trend (Figs. 26.5 and 26.7b). One should note that the inter-annual variability for our study region is large compared to the magnitudes of these trends and so, when tested, these

trends did not show statistical significance. This is consistent with other results that have pointed out that vegetation trends are mostly not statistically significant for our study region and the MODIS operational period (Samanta et al. 2011; Cortés et al. 2021). However, an examination of the trends plotted spatially on a per gridcell basis (Fig. 26.6a) shows regional hotspots of statistical significant greening and browning. Furthermore it should be noted that even within a particular biome, different regions can show opposite trends (consider, for example, LPJ-GUESS in the western and eastern parts of the Fynbos biome in Fig. 26.6a) which is not apparent from the biome averaged results (Fig. 26.4). The LPJ-GUESS derived NPP over the whole southern Africa region shows a statistically significant rise since 1901 but with high IAV and decadal scale fluctuations due to internal climate variability or oscillations. Therefore, we can conclude the future NPP trajectory will be governed by both climate variability and long-term trends resulting from changing drivers due to global change.

26.4.2 Drivers of NPP Patterns and Trends

The spatial pattern of NPP, shorter-term temporal trends, and inter-annual variability appear to be mainly driven by gradients or changes in precipitation (Figs. 26.2, 26.4, and 26.8). This can be seen, for example, with the high NPP occurring along the eastern coastal parts of the region (Fig. 26.2). This region receives the highest rainfall while the western and central part of the region experiences high temperatures and less rainfall (Botai et al. 2018). As outlined in the introduction, we expected this dominant role of precipitation as a driver of NPP variations. This is in agreement with the study conducted by Zhu et al. 2016, where they concluded that the greening in South Africa over the period from 1982 to 2009 is primarily driven by increasing precipitation. Recent climate projections show decreasing precipitation trends in southern Africa both for low and high warming scenarios, with corresponding increases in aridity and drought (IPCC 2021). Higher levels of warming result in stronger precipitation decreases, with the highest percentage decreases projected in the west of the region, which is already arid (IPCC 2021, Fig. SPM.5c). Our results indicate that, up to 2015, precipitation decreases have not yet caused widespread negative impacts on NPP as we can see slightly increasing trends in Figs. 26.4 and 26.7a, although there are some regional exceptions (Fig. 26.6a). The potential effects of future drying on NPP and the consequences for ecosystems, ecosystem services, agriculture, and forestry remain an open question. To tackle this question, predictive methods such as DGVMs, with more detailed or regionally parameterized representations of land-use, or more empirical modelling approaches must be applied in combination with future climate projections and, ideally, informed by experimental work.

The observed high negative correlation with solar radiation is likely due to the fact that precipitation is associated with cloud cover and therefore decreased solar radiation. This indicates that whilst solar radiation is essential for photosynthesis and therefore NPP, it is not a limiting factor to the same degree as precipitation and

so is in fact not a driver of NPP in the study region (Nemani et al. 2003). The same was found by Hickler et al. (2005) (Fig. 3) for the Sahel region.

In our study region, NPP shows a negative correlation with temperature. This is consistent with the fact that most of the study region is in the subtropical to warm temperate climate zones, so photosynthesis is unlikely to be temperature limited (not applicable for winter rain regions in the south west) and no positive correlation is expected (Nemani et al. 2003). Instead, this negative correlation may occur due to a combination of increased autotrophic respiration rates that accompany higher temperatures, a net reduction of photosynthesis due to decreased efficiency and heat stress at higher temperatures, and decreased soil water availability due to stronger atmospheric moisture demand. Among all the climatic variables analysed, only temperature in the Succulent Karoo and Desert biome showed statistically significant trends (increasing) from 2002 to 2015. Taking these findings together and putting them in the context of global change, it is likely that temperature will have an escalating and negative effect on NPP in these biomes in the coming decades, at least under moderate warming without unprecedented heat stress for the vegetation, which is not represented in the applied model version.

According to LPJ-GUESS, the plant-physiological effects of increasing atmospheric CO₂ have been large and positive between 1901 and 2015 (Fig. 26.7a). However, the simulated CO₂ effects over the last decades are only minor in similar arid environments (Hickler et al. 2005). The strong effects since the beginning of the last century are consistent with other global estimates. Ciais et al. (2012) estimated a pre-industrial GPP of 80 Pg year⁻¹, which is substantially lower than the present estimate of about 120 Pg (Ciais et al., 2013; Friedlingstein et al., 2020). Using another independent method, Campbell et al. (2017) estimated a GPP increase of about 31% since the early last century. GPP and NPP are strongly related, NPP being about half of GPP (Ciais et al., 2013; Yu et al., 2018), which also applies to LPJ-GUESS (Ardö 2015). The CO₂ effect is also in line with a global greening trend attribution study using different leaf area index (LAI) estimates and ten DGVMs (Zhu et al. 2016). These authors concluded that CO₂ fertilisation explains 70% of the observed greening trend between 1982 and 2009, particularly in the tropics. Their analyses, however, suggested other major drivers for most of southern Africa, namely climate change in the north-eastern part of our study region and land cover change in central South Africa (Zhu et al. 2016; Fig. 26.3c). In our study region, CO₂ effects have been found to be minor under extreme drought stress when meristem growth is strongly limited by leaf turgor (Xu et al., 2016). Moreover, future CO₂ fertilisation effects might be smaller as the CO₂ limitation of photosynthesis increasingly saturates and because of progressive nutrient limitation (Hickler et al. 2015; Wang et al. 2020).

26.5 Conclusion

The two rather independent approaches to estimate spatial patterns and recent past trends in NPP we used (Earth-observation-based estimations from MODIS and the LPJ-GUESS DGVM) provided similar results. This suggests that the spatio-temporal results presented here are robust. As the MODIS estimate is more constrained by observed data, this result may also be considered as an evaluation of the LPJ-GUESS model. Thus, the model should be suitable for future projections in southern Africa in order to inform climate adaptation and mitigation measures.

Precipitation change is the most important driver of NPP dynamics in the study region, particularly of the inter-annual variations and spatial distribution. However, increasing atmospheric CO₂ has had a large effect since the early twentieth century and might continue to play a significant role as anthropogenic CO₂ emissions continue. Solar radiation and temperature were not found to be significant drivers of NPP in the study region.

Given the importance of precipitation in southern Africa and its projected decline, it is likely that ecosystems and agriculture will be under increasing pressure as their foundational building block, NPP, might decrease in areas where precipitation strongly decreases. The findings presented here alert us of the importance of mitigation and adaptation strategies going into the future and the challenges global change will bring. Both simulation models and Earth observation data can play an important role in meeting these challenges.

Acknowledgements The authors would like to thank Prof. Dr. Lukas Lehnert, from Ludwig-Maximilians University in Munich, Germany, for his comments regarding trends on remote sensing data. The authors further like to extend their gratitude to Dr. Jasper Slingsby from the University of Cape Town, South Africa and their anonymous reviewer for their constructive and insightful comments which significantly improved their chapter.

References

- Abdi AM, Seaquist J, Tenenbaum DE, Eklundh L, Ardö J (2014) The supply and demand of net primary production in the Sahel. *Environ Res Lett* 9(9). <https://doi.org/10.1088/1748-9326/9/9/094003>
- Andersen CB, Quinn J (2020) Human appropriation of net primary production. *Encycl World's Biomes*:22–28. <https://doi.org/10.1016/B978-0-12-409548-9.12434-0>
- Archibald SA, Kirton A, Van Der Merwe MR, Scholes RJ, Williams CA, Hanan N (2009) Drivers of inter-annual variability in Net Ecosystem Exchange in a semi-arid savanna ecosystem, South Africa. *Biogeosciences* 6(2):251–266. <https://doi.org/10.5194/bg-6-251-2009>
- Ardö J (2015) Comparison between remote sensing and a dynamic vegetation model for estimating terrestrial primary production of Africa. *Carbon Balance Manag* 10(1). <https://doi.org/10.1186/s13021-015-0018-5>
- Bondeau A, Smith P, Zaehle S, Schaphoff S, Lucht W, Cramer W, Gerten D, Lotze-Campen H, Müller C, Reichstein M, Smith B (2007) Modelling the role of agriculture for the 20th century global terrestrial carbon balance. *Glob Change Biol* 13:679–706
- Bon-Gang H (2018) Methodology. In: Performance and improvement of green construction projects. Elsevier, pp 15–22

- Botai CM, Botai JO, Adeola AM (2018) Spatial distribution of temporal precipitation contrasts in South Africa. *S Afr J Sci* 114(7–8):1–9. <https://doi.org/10.17159/sajs.2018/20170391>
- Campbell JE, Berry JA, Seibt U, Smith SJ, Montzka SA, Launois T, Belviso S, Bopp L, Laine M (2017) Large historical growth in global terrestrial gross primary production. *Nature* 544(7648):84–87. <https://doi.org/10.1038/NATURE22030>
- Cao Z (2020) Chapter 9 – Assessment methods for air pollution exposure. In: Li L, Zhou X, Tong W (eds) *Spatiotemporal analysis of air pollution and its application in public health*. Elsevier, pp 197–206., ISBN 9780128158227. <https://doi.org/10.1016/B978-0-12-815822-7.00009-1>
- Chapin FS, Matson PA, Vitousek PM (2011) *Principles of terrestrial ecosystem ecology*. <https://doi.org/10.1007/978-1-4419-9504-9>
- Ciais P, Tagliabue A, Cuntz M, Bopp L, Scholze M, Hoffmann G, Lourantou A, Harrison SP, Prentice IC, Kelley DI, Koven C, Piao SL (2012) Large inert carbon pool in the terrestrial biosphere during the Last Glacial Maximum. *Nat Geosci* 5(1):74–79. <https://doi.org/10.1038/ngeo1324>
- Ciais P, Sabine C, Bala G, Bopp L, Brovkin V, Canadell J, Chhabra A, DeFries R, Galloway J, Heimann M, Jones C, Le Quéré C, Myneni RB, Piao S, Thornton P (2013) Carbon and other biogeochemical cycles. In: Stocker TF, Qin D, Plattner G-K, Tignor M, Allen SK, Boschung J, Nauels A, Xia Y, Bex V, Midgley PM (eds) *Climate Change 2013 The physical science basis. Contribution of working group I to the fifth assessment report of the intergovernmental panel on climate change*. Cambridge University Press, Cambridge, pp 465–570. <https://doi.org/10.1017/CBO9781107415324.015>
- Clark DA, Brown S, Kicklighter DW, Chambers JQ, Thomlinson JR, Ni J (2001) Measuring net primary production in forests: concepts and field methods. *Ecol Appl* 11(2):356–370
- Cooper JJ, Fleming GJ, Malungani TP, Misselhorn AA (2004) Ecosystem services in Southern Africa: a regional assessment
- Cortes J, Mahecha MD, Reichstein M, Myneni RB, Chen C, Brenning A (2021) Where are global vegetation greening and browning trends significant? *Geophys Res Lett* 48:9
- Cui T, Wang Y, Sun R, Qiao C, Fan W, Jiang G, Hao L, Zhang L (2016) Estimating vegetation primary production in the Heihe River Basin of China with multi-source and multi-scale data. *PLoS One* 11(4):153971. <https://doi.org/10.1371/journal.pone.0153971>
- Daron J (2015) Challenges in using a Robust Decision Making approach to guide climate change adaptation in South Africa. *Clim Change* 132(3):459–473. <https://doi.org/10.1007/s10584-014-1242-9>
- Didan K (2015) MOD13C2 MODIS/Terra Vegetation Indices Monthly L3 Global 0.05Deg CMG. NASA LP DAAC. <https://doi.org/10.5067/MODIS/MOD13C2.006>
- Dyson LL, van Heerden J (2001) The heavy rainfall and floods over the northeastern interior of South Africa during February 2000. *South African Journal of Science* 97(3):80–86
- Drüke M, Von Bloh W, Petri S, Sakschewski B, Schaphoff S, Forkel M, Huiskamp W, Feulner G, Thonicke K (2021) CM2Mc-LPJmL v1.0: Biophysical coupling of a process-based dynamic vegetation model with managed land to a general circulation model. *Geosci Model Dev* 14(6):4117–4141. <https://doi.org/10.5194/GMD-14-4117-2021>
- Feng Y, Zhu J, Zhao X, Tang Z, Zhu J, Fang J (2019) Changes in the trends of vegetation net primary productivity in China between 1982 and 2015. *Environ Res Lett* 14(12):124009. <https://doi.org/10.1088/1748-9326/AB4CD8>
- Fetzel T, Niederscheider M, Erb K-H, Gaube V, Gingrich S, Haberl H, Krausmann F, Lauk C, Plutzer C (2012) Human appropriation of net primary production in Africa: patterns, trajectories, processes and policy implications. *Soc Ecol Work Pap* 37(August):725
- Forkel M, Carvalhais N, Verbesselt J, Mahecha MD, Neigh CSR, Reichstein M (2013) Trend change detection in NDVI time series: effects of inter-annual variability and methodology. *Remote Sens* 5(5):2113–2144. <https://doi.org/10.3390/rs5052113>
- Friedlingstein P, O'Sullivan M, Jones MW, Andrew RM, Hauck J, Olsen A, Peters GP, Peters W, Pongratz J, Sitch S, Le Quéré C, Canadell JG, Ciais P, Jackson RB, Alin S, Aragão LEOC, Arneeth A, Arora V, Bates NR, Becker M, Benoit-Cattin A, Bittig HC, Bopp L, Bultan S, Chandra N, Chevallier F, Chini LP, Evans W, Florentie L, Forster PM, Gasser T, Gehlen M,

- Gilfillan D, Gkritzalis T, Gregor L, Gruber N, Harris I, Hartung K, Haverd V, Houghton RA, Ilyina T, Jain AK, Joetzer E, Kadono K, Kato E, Kitidis V, Korsbakken JI, Landschützer P, Lefèvre N, Lenton A, Lienert S, Liu Z, Lombardozi D, Marland G, Metz N, Munro DR, Nabel JEMS, Nakaoka SI, Niwa Y, O'Brien K, Ono T, Palmer PI, Pierrot D, Poulter B, Resplandy L, Robertson E, Rödenbeck C, Schwinger J, Séférian R, Skjelvan I, Smith AJP, Sutton AJ, Tanhua T, Tans PP, Tian H, Tilbrook B, Van Der Werf G, Vuichard N, Walker AP, Wanninkhof R, Watson AJ, Willis D, Wiltshire AJ, Yuan W, Yue X, Zaehle S (2020) Global Carbon Budget (2020). *Earth Syst Sci Data* 12(4):3269–3340. <https://doi.org/10.5194/essd-12-3269-2020>
- Fukano Y, Guo W, Aoki N, Ootsuka S, Noshita K, Uchida K, Kato Y, Sasaki K, Kamikawa S, Kubota H (2021) GIS-based analysis for UAV-supported field experiments reveals soybean traits associated with rotational benefit. *Front Plant Sci* 0:1003. <https://doi.org/10.3389/FPLS.2021.637694>
- Gao Y, Zhou X, Wang Q, Wang C, Zhan Z, Chen L, Yan J, Qu R (2013) Vegetation net primary productivity and its response to climate change during 2001–2008 in the Tibetan Plateau. *Sci Total Environ* 444:356–362. <https://doi.org/10.1016/j.scitotenv.2012.12.014>
- Gao Q, Guo Y, Xu H, Ganjurjav H, Li Y, Wan Y, Qin X, Ma X, Liu S (2016) Climate change and its impacts on vegetation distribution and net primary productivity of the alpine ecosystem in the Qinghai-Tibetan Plateau. <https://doi.org/10.1016/j.scitotenv.2016.02.131>
- Gerten D, Schaphoff S, Haberlandt U, Lucht W, Sitch S (2004) Terrestrial vegetation and water balance-hydrological evaluation of a dynamic global vegetation model. <https://doi.org/10.1016/j.jhydrol.2003.09.029>
- Gonsamo A, Chen JM (2017) 3.11 – Vegetation primary productivity. In: Liang S (ed) *Comprehensive remote sensing*. Elsevier, pp 163–189. <https://doi.org/10.1016/B978-0-12-409548-9.10535-4>. ISBN 9780128032213
- Gonzalez-Meler MA, Taneva L, Trueman RJ (2004) Plant respiration and elevated atmospheric CO₂ concentration: cellular responses and global significance. *Ann Bot* 94:647–656. <https://doi.org/10.1093/aob/mch189>
- Gornall J, Betts R, Burke E, Clark R, Camp J, Willett K, Wiltshire A (2010) Implications of climate change for agricultural productivity in the early twenty-first century. *Philos Trans R Soc B Biol Sci* 365:2973–2989. <https://doi.org/10.1098/rstb.2010.0158>
- Gulev SK, Thorne PW, Ahn J, Dentener FJ, Domingues CM, Gerland S, Gong D, Kaufman DS, Nnamchi HC, Quaas J, Rivera JA, Sathyendranath S, Smith SL, Trewin B, von Shuckmann K, Vose RS (2021) Changing state of the climate system. In: Masson Delmotte V, Zhai P, Pirani A, Connors SL, Péan C, Berger S, Caud N, Chen Y, Goldfarb L, Gomis MI, Huang M, Leitzell K, Lonnoy E, Matthews JBR, Maycock TK, Waterfield T, Yelekçi O, Yu R, Zhou B (eds) *Climate Change 2021: The Physical Science Basis. Contribution of Working Group I to the Sixth Assessment Report of the Intergovernmental Panel on Climate Change*. Cambridge University Press. In Press
- Haberl H, Erb KH, Krausmann F, Gaube V, Bondeau A, Plutzar C, Gingrich S, Lucht W, Fischer-Kowalski M (2007) Quantifying and mapping the human appropriation of net primary production in earth's terrestrial ecosystems. *Proc Natl Acad Sci* 104(31):12942–12947. <https://doi.org/10.1073/PNAS.0704243104>
- Hantson S, Arnett A, Harrison SP, Kelley DI, Prentice IC, Rabin SS, Archibald S, Mouillot F, Arnold SR, Artaxo P, Bachelet D, Ciais P, Forrest M, Friedlingstein P, Hickler T, Kaplan JO, Kloster S, Knorr W, Lasslop G, Li F, Mangeon S, Melton JR, Meyn A, Sitch S, Spessa A, van der Werf GR, Voulgarakis A, Yue C (2016) The status and challenge of global fire modelling. *Biogeosciences* 13:3359–3375. <https://doi.org/10.5194/bg-13-3359-2016>
- Harada Y, Kamahori H, Kobayashi C, Endo H, Kobayashi S, Ota Y, Onoda H, Onogi K, Miyaoka K, Takahashi K (2016) The JRA-55 reanalysis: representation of atmospheric circulation and climate variability. *J Meteorol Soc Jpn Ser II* 94:269–302. <https://doi.org/10.2151/jmsj.2016-015>
- Harris IC, Jones PD (2019) CRU TS3.26: Climatic Research Unit (CRU) Time-Series (TS) Version 3.26 of High-resolution gridded data of month-by-month variation in climate (Jan. 1901–Dec.

- 2017). Centre for Environmental Data Analysis, 01 March 2019. <https://dx.doi.org/10.5285/7ad889f2cc1647efba7e6a356098e4f3>
- Hazarika MK, Yasuoka Y, Ito A, Dye D (2005) Estimation of net primary productivity by integrating remote sensing data with an ecosystem model. *Remote Sens Environ* 94(3):298–310. <https://doi.org/10.1016/j.rse.2004.10.004>
- Heisler-White JL, Knapp AK, Kelly EF (2008) Increasing precipitation event size increases aboveground net primary productivity in a semi-arid grassland. *Oecologia* 158(1):129–140. <https://doi.org/10.1007/s00442-008-1116-9>
- Hickler T, Eklundh L, Seaquist JW, Smith B, Ardo J, Olsson L, Sykes MT, Sjo M (2005) Precipitation controls Sahel greening trend. *Geophys Res Lett* 32:2–5. <https://doi.org/10.1029/2005GL024370>
- Hickler T, Rammig A, Werner C (2015) Modelling CO2 impacts on forest productivity. *Curr For Rep* 1(2):69–80. <https://doi.org/10.1007/s40725-015-0014-8>
- Higginbottom TP, Symeonakis E (2014) Assessing land degradation and desertification using vegetation index data: current frameworks and future directions. *Remote Sens* 6(10):9552–9575. <https://doi.org/10.3390/rs6109552>
- Hurt GC, Chini LP, Froelking S, Betts RA, Feddema J, Fischer G, Fisk JP, Hibbard K, Houghton RA, Janetos A, Jones CD, Kindermann G, Kinoshita T, Klein Goldewijk K, Riahi K, Shevliakova E, Smith S, Stehfest E, Thomson A, Thornton P, van Vuuren DP, Wang YP (2011) Harmonization of land-use scenarios for the period 1500–2100: 600 years of global gridded annual land-use transitions, wood harvest, and resulting secondary lands. *Clim Change* 109:117. <https://doi.org/10.1007/s10584-011-0153-2>
- IPCC (2021) Summary for policymakers. In: Masson Delmotte V, Zhai P, Pirani A, Connors SL, Péan C, Berger S, Caud N, Chen Y, Goldfarb L, Gomis MI, Huang M, Leitzell K, Lonnoy E, Matthews JBR, Maycock TK, Waterfield T, Yelekçi O, Yu R, Zhou B (eds) *Climate Change 2021: The Physical Science Basis. Contribution of Working Group I to the Sixth Assessment Report of the Intergovernmental Panel on Climate Change*. Cambridge University Press. In Press
- Ji Y, Zhou G, Luo T, Dan Y, Zhou L, Lv X (2020) Variation of net primary productivity and its drivers in China's forests during 2000–2018. *For Ecosyst* 7(1):1–11. <https://doi.org/10.1186/S40663-020-00229-0>
- Jung M, Reichstein M, Bondeau A (2009) Towards global empirical upscaling of FLUXNET eddy covariance observations: validation of a model tree ensemble approach using a biosphere model. *Biogeosciences* 6:2001–2013
- Kelley DI, Prentice I, Harrison S, Wang H, Simard M, Fisher JB, Willis K (2013) A comprehensive benchmarking system for evaluating global vegetation models. *Biogeosciences* 10:3313–3340. <https://doi.org/10.5194/bg-10-3313-2013>
- Knorr W, Arneth A, Jiang L (2016) Demographic controls of future global fire risk. *Nature Clim Change* 6:781–785. <https://doi.org/10.1038/nclimate2999>
- Kidwell KB (comp, ed) (1995) NOAA Polar Orbiter Data (TIROS-N, NOAA-6, NOAA-7, NOAA-8, NOAA-9, NOAA-10, NOAA-11, NOAA-12, and NOAA-14, NOAA-15, NOAA-16, NOAA-17, NOAA-18, NOAA-19) Users Guide NOAA/NESDIS, Washington, D.C.
- Kobayashi S, Ota Y, Harada Y, Ebata A, Moriya M, Onoda H, Onogi K, Kamahori H, Kobayashi C, Endo H, Miyaoka K, Kiyotoshi T (2015) The JRA-55 reanalysis: general specifications and basic characteristics. *J Meteorol Soc Jpn* 93(1):5–48. <https://doi.org/10.2151/jmsj.2015-001>
- Lindeskog M, Arneth A, Bondeau A, Waha K, Seaquist J, Olin S, Smith B (2013) Implications of accounting for land use in simulations of ecosystem carbon cycling in Africa. *Earth Syst Dyn* 4(2):385–407. <https://doi.org/10.5194/esd-4-385-2013>
- Liu Y, Kumar M, Katul GG, Porporato A (2019) Reduced resilience as an early warning signal of forest mortality. *Nat Clim Chang* 9:880–885. <https://doi.org/10.1038/s41558-019-0583-9>
- Luo T, Pan Y, Ouyang H, Shi P, Luo J, Yu Z, Lu Q (2004) Leaf area index and net primary productivity along subtropical to alpine gradients in the Tibetan Plateau. *Glob Ecol Biogeogr* 13(4):345–358. <https://doi.org/10.1111/j.1466-822X.2004.00094.x>

- Malherbe J, Dieppois B, Maluleke P, Van Staden M, Pillay DL (2015) South African droughts and decadal variability. *Nat Hazards* 80(1):657–681. <https://doi.org/10.1007/S11069-015-1989-Y>
- Mann HB (1945) Non-parametric tests against trend. *Econometrica* 13:245–259
- Masoudi M, Jokar P, Pradhan B (2018) A new approach for land degradation and desertification assessment using geospatial techniques. *Hazards Earth Syst Sci* 18:1133–1140. <https://doi.org/10.5194/nhess-18-1133-2018>
- Mattiuzzi M, Verbesselt J, Hengl T, Klisch A, Stevens F, Mosher S, Evans B, Lobo A, Hufkens K, Detsch F (2017) MODIS – acquisition and processing of MODIS products. <https://github.com/MatMatt/MODIS>
- Medlyn BE (2011) Comment on “Drought-induced reduction in global terrestrial net primary production from 2000 through 2009”. *Science* 333:1
- Melillo JM, McGuire AD, Kicklighter DW, Moore B, Vorosmarty CJ, Schloss AL (1993) Global climate change and terrestrial net primary production. *Nature* 363(6426):234–240. <https://doi.org/10.1038/363234a0>
- Midgley GF, Bond WJ (2015) Future of African terrestrial biodiversity and ecosystems under anthropogenic climate change. *Nat Clim Change* 5:823–829. <https://doi.org/10.1038/nclimate2753>
- Minnett PJ (2001) Satellite remote sensing of sea surface temperatures. *Encycl Ocean Sci*:91–102. <https://doi.org/10.1016/b978-012374473-9.00343-x>
- Mohamed MAA, Babiker IS, Chen ZM, Ikeda K, Ohta K, Kato K (2004) The role of climate variability in the inter-annual variation of terrestrial net primary production (NPP). *Sci Total Environ* 332:123–137. <https://doi.org/10.1016/j.scitotenv.2004.03.009>
- Monteith J (1972) Solar radiation and productivity in tropical ecosystems. *J Appl Ecol* 9(3):747–766
- Myneni RB, Knyazikhin Y, Privette JL, Running SW, Nemani R, Zhang Y, Tian Y, Wang Y, Morisette JT, Glassy J, Votava P (1999) MODIS Leaf Area Index (LAI) and fraction of photosynthetically active radiation absorbed by vegetation (FPAR) product. *Modis Atbd Version 4*.(4.0):130
- Myneni RB, Hoffman S, Knyazikhin Y, Privette JL, Glassy J, Tian Y, Wang Y, Song X, Zhang Y, Smith GR, Lotsch A, Friedl M, Morisette JT, Votava P, Nemani RR, Running SW (2002) Global products of vegetation leaf area and fraction absorbed PAR from year one of MODIS data. *Remote Sens Environ* 83(1–2):214–231. [https://doi.org/10.1016/S0034-4257\(02\)00074-3](https://doi.org/10.1016/S0034-4257(02)00074-3)
- Nemani RR, Keeling CD, Hashimoto H, Jolly WM, Piper SC, Tucker CJ, Myneni RB, Running SW (2003) Climate-driven increases in global terrestrial net primary production from 1982 to 1999. *Science* 300(5625):1560–1563. <https://doi.org/10.1126/science.1082750>
- Niedertscheider M (2011) Human appropriation of net primary production in South Africa, 1961–2006. A socio-ecological analysis. Master thesis, Vienna University, Vienna
- Nieradzki LP, Haverd VE, Briggs P, Meyer CP, Canadell J (2015) BLAZE, a novel Fire-model for the CABLE Land-surface model applied to a Re-assessment of the Australian continental carbon budget. *AGU Fall Meeting Abstracts* December 14–18
- Pachavo G, Murwira A (2014) Remote sensing net primary productivity (NPP) estimation with the aid of GIS modelled shortwave radiation (SWR) in a Southern African Savanna. *Int J Appl Earth Obs Geoinf* 30(1):217–226. <https://doi.org/10.1016/J.JAG.2014.02.007>
- Pan S, Dangal SRS, Tao B, Yang J, Tian H (2015) Recent patterns of terrestrial net primary production in Africa influenced by multiple environmental changes. *Ecosyst Heal Sustain* 1(5):1–15. <https://doi.org/10.1890/EHS14-0027.1>
- Peng D, Zhang B, Wu C, Huete AR, Gonsamo A, Lei L, Ponce-Campos GE, Liu X, Wu Y (2017) Country-level net primary production distribution and response to drought and land cover change. *Sci Total Environ* 574:65–77. <https://doi.org/10.1016/j.scitotenv.2016.09.033>
- Peterson BG, Carl P, Boudt K, Bennett R, Ulrich J, Zivot E, Cornilly D (2020) “Performance-Analytics” Econometric tools for performance and risk analysis. <https://github.com/braverock/PerformanceAnalytics>

- Portmann FT, Siebert S, Döll P (2010) MIRCA2000—Global monthly irrigated and rainfed crop areas around the year 2000: a new high-resolution data set for agricultural and hydrological modeling. *Glob Biogeochem Cycle* 24. <https://doi.org/10.1029/2008GB003435>
- Prentice IC, Bondeau A, Cramer W, Harrison SP, Hickler T, Lucht W, Sitch S, Smith B, Sykes MT (2007) Dynamic global vegetation modelling: quantifying terrestrial ecosystem responses to large-scale environmental change. In: Canadell JD, Pataki E, Pitelka LF (eds) *Terrestrial ecosystems in a changing world*. Springer, Berlin, pp 175–192
- Pugh TAM, Lindeskog M, Smith B, Poulter B, Arneth A, Haverd V, Calle L (2019) Role of forest regrowth in global carbon sink dynamics. *Proc Natl Acad Sci U S A* 116:4382–4387
- Ranasinghe R, Ruane AC, Vautard R, Arnell N, Coppola E, Cruz FA, Dessai S, Islam AS, Rahimi M, Carrascal DR, Sillmann J, Sylla MB, Tebaldi C, Wang W, Zaaboul R (2021) Climate change information for regional impact and for risk assessment. In: Masson Delmotte V, Zhai P, Pirani A, Connors SL, Péan C, Berger S, Caud N, Chen Y, Goldfarb L, Gomis MI, Huang M, Leitzell K, Lonnoy E, Matthews JBR, Maycock TK, Waterfield T, Yelekçi O, Yu R, Zhou B (eds) *Climate Change 2021: The Physical Science Basis. Contribution of Working Group I to the Sixth Assessment Report of the Intergovernmental Panel on Climate Change*. Cambridge University Press. In Press
- Reeves MC, Moreno AL, Bagne KE, Running SW (2014) Estimating climate change effects on net primary production of rangelands in the United States. *Clim Change* 126(3–4):429–442. <https://doi.org/10.1007/s10584-014-1235-8>
- Ruimy A, Saugier B, Dedieu G (1994) Methodology for the estimation of terrestrial net primary production from remotely sensed data. *J Geophys Res* 99(D3):5263–5283. <https://doi.org/10.1029/93JD03221>
- Running SW, Nemani RR, Heinsch FA, Zhao M, Reeves M, Hashimoto H (2004) A continuous satellite-derived measure of global terrestrial primary production. *BioScience* 54(6):547–560. [https://doi.org/10.1641/0006-3568\(2004\)054\[0547:ACSMOG\]2.0.CO;2](https://doi.org/10.1641/0006-3568(2004)054[0547:ACSMOG]2.0.CO;2)
- Rutherford MC, Mucina L, Powrie LW (2006) Biomes and bioregions of southern Africa: the vegetation of South Africa, Lesotho and Swaziland. *Strelitzia* 19:31–51
- Sala OE, Austin AT (2000) Methods of estimating aboveground net primary productivity. In: Sala OE, Jackson RB, Mooney HA, Howarth RW (eds) *Methods in ecosystem science*. Springer, New York, pp 31–43
- Samanta A, Costa MH, Nunes EL, Vieira SA, Xu L, Myneni RB (2011) Comment on “Drought-induced reduction in global terrestrial net primary production from 2000 through 2009”. *Science* 333:2
- Savtchenko A, Ouzounov D, Ahmad S, Acker J, Leptoukh G, Koziara J, Nickless D (2004) Terra and Aqua MODIS products available from NASA GES DAAC. *Adv Sp Res* 34(4):710–714. <https://doi.org/10.1016/j.asr.2004.03.012>
- Schoeman CM, Monadjem A (2018) Community structure of bats in the savannas of southern Africa: influence of scale and human land use. *Hystrix, Ital J Mammal* 29(1):3–10. <https://doi.org/10.4404/hystrix-00038-2017>
- Seauquist JW, Hickler T, Eklundh L, Ardö J, Heumann BW (2008) Disentangling the effects of climate and people on Sahel vegetation dynamics. *Biogeosci Discuss* 5(4):3045–3067. <https://doi.org/10.5194/bgd-5-3045-2008>
- Simmons A, Fellous JL, Ramaswamy V, Trenberth K, Asrar G, Burrows JP, Ciaia P, Drinkwater M, Friedlingstein P, Gobron N, Guilyardi E, Halpern D, Heimann M, Johannessen J, Levelt PF, Lopez-Baeza E, Penner J, Scholes R, Shepherd T (2016) Observation and integrated Earth system science: a roadmap for 2016–2025. *Adv Space Res* 57:2037–2103. <https://doi.org/10.1016/j.asr.2016.03.008>
- Sitch S, Smith B, Prentice IC, Arneth A, Bondeau A, Cramer W, Kaplan JO, Levis S, Lucht W, Sykes MT, Thonicke K, Venevsky S (2003) Evaluation of ecosystem dynamics, plant geography and terrestrial carbon cycling in the LPJ dynamic global vegetation model. *Glob Chang Biol* 9(2):161–185. <https://doi.org/10.1046/j.1365-2486.2003.00569.x>
- Sitch S, Huntingford C, Gedney N, Levy PE, Lomas M, Piao SL, Betts R, Ciaia P, Cox P, Friedlingstein P, Jones CD, Prentice IC, Woodward FI (2008) Evaluation of the terrestrial carbon

- cycle, future plant geography and climate-carbon cycle feedbacks using five dynamic global vegetation models (DGVMs). *Glob Change Biol* 14(9):2015–2039. <https://doi.org/10.1111/j.1365-2486.2008.01626.x>
- Smith B (2001) LPJ-GUESS – an ecosystem modelling framework. *Dep Phys Geogr Ecosyst Anal INES, Sölvegatan* 12:22362
- Smith B, Wärlind D, Arneth A, Hickler T, Leadley P, Siltberg J, Zaehle S (2014) Implications of incorporating N cycling and N limitations on primary production in an individual-based dynamic vegetation model. *Biogeosciences* 11(7):2027–2054. <https://doi.org/10.5194/bg-11-2027-2014>
- Smith B, Prentice IC, Sykes MT (2001) Representation of vegetation dynamics in the modelling of terrestrial ecosystems: comparing two contrasting approaches within European climate space. *Glob Ecol Biogeogr* 10:621–637
- Smithers JC, Schulze RE, Pike A, Jewitt GPW (2001) A hydrological perspective of the February 2000 floods : a case study in the Sabie River catchment. *Water SA*, 27(3):325–332. <https://doi.org/doi:10.4314/wsa.v27i3.4975>
- Solano R, Didan K, Jacobson A, Huete A (2010) MODIS Vegetation Index User's Guide (MOD13 Series). Univ Arizona 2010(May):38
- Sus O, Stengel M, Stapelberg S, McGarragh G, Poulsen C, Povey AC, Schlundt TG, Christensen M, Proud S, Jerg M, Grainger R, Hollmann R (2018) The Community Cloud retrieval for CLimate (CC4CL) – Part 1: A framework applied to multiple satellite imaging sensors. *Atmos Measur Tech* 11:3373–3396
- Tao B, Li K, Shao X, Cao M (2003) The temporal and spatial patterns of terrestrial net primary productivity in China. *J Geogr Sci* 13(2):163–171. <https://doi.org/10.1007/bf02837454>
- Trishchenko AP, Fedosejevs G, Li Z, Cihlar J (2002) Trends and uncertainties in thermal calibration of AVHRR radiometers onboard NOAA-9 to NOAA-16. *J Geophys Res Atmos* 107(24):ACL 17-1–ACL 17-13. <https://doi.org/10.1029/2002JD002353>
- Tucker CJ (1979) Red and photographic infrared linear combinations for monitoring vegetation. *Remote Sens Environ* 8(2):127–150. [https://doi.org/10.1016/0034-4257\(79\)90013-0](https://doi.org/10.1016/0034-4257(79)90013-0)
- Urban M, Forkel M, Schimmlius C, Hese S, Hüttich C, Herold M (2013) Identification of land surface temperature and albedo trends in AVHRR Pathfinder data from 1982 to 2005 for northern Siberia. *Int J Remote Sens* 34(12):4491–4507. <https://doi.org/10.1080/01431161.2013.779760>
- Wang S, Zhang Y, Ju W, Chen JM, Ciaia P, Cescatti A, Sardans J, Janssens IA, Wu M, Berry JA, Campbell E, Fernández-Martínez M, Alkama R, Sitch S, Friedlingstein P, Smith WK, Yuan W, He W, Lombardo D, Kautz M, Zhu D, Lienert S, Kato E, Poulter B, Sanders TGM, Krüger I, Wang R, Zeng N, Tian H, Vuichard N, Jain AK, Wiltshire A, Haverd V, Goll DS, Peñuelas J (2020) Recent global decline of CO₂ fertilization effects on vegetation photosynthesis. *Science* 370(6522):1295–1300. <https://doi.org/10.1126/science.abb7772>
- Wickham H (2016) *ggplot2: Elegant graphics for data analysis*. Springer, New York. ISBN 978-3-319-24277-4. <https://ggplot2.tidyverse.org>
- Xiao J, Zhuang Q, Baldocchi DD, Law BE, Richardson AD, Chen J, Oren R, Starr G, Noormets A, Ma S, Verma SB, Wharton S, Wofsy SC, Bolstad PV, Burns SP, Cook DR, Curtis PS, Drake BG, Falk M, Fischer ML, Foster DR, Gu L, Hadley JL, Hollinger DY, Katul GG, Litvak M, Martin TA, Matamala R, McNulty S, Meyers TP, Monson RK, Munger JW, Oechel WC, Tha Paw U K, Schmid HP, Scott RL, Sun G, Suyker AE, Torn MS (2008) Estimation of net ecosystem carbon exchange for the conterminous United States by combining MODIS and AmeriFlux data. *148(11):1827–1847*. <https://doi.org/10.1016/j.agrformet.2008.06.015>
- Xiao X, Doughty R, Wu X, Zhang Y, Chang Q, Qin Y, Wang J, Bajgain R (2019) Spatial-temporal dynamics of global terrestrial gross primary production during 2000-2018: an update on vegetation photosynthesis model and its simulations with Terra/MODIS images. American Geophysical Union, Fall Meeting 2019
- Xu Z, Jiang Y, Jia B, Zhou G (2016) Elevated-CO₂ response of stomata and its dependence on environmental factors. *Front Plant Sci* 7(657). <https://doi.org/10.3389/fpls.2016.00657>

- Yang W, Shabanov NV, Huang D, Wang W, Dickinson RE, Nemani RR, Knyazikhin Y, Myneni RB (2006) Analysis of leaf area index products from combination of MODIS Terra and Aqua data. *Remote Sens Environ* 104:297–312. <https://doi.org/10.1016/j.rse.2006.04.016>
- Yu T, Sun R, Xiao Z, Zhang Q, Liu G, Cui T, Wang J (2018) Estimation of global vegetation productivity from Global LAnd Surface Satellite data. *Remote Sens* 10(2). <https://doi.org/10.3390/rs10020327>
- Zaehle S, Friedlingstein P, Friend AD (2010) Terrestrial nitrogen feedbacks may accelerate future climate change. *Geophys Res Lett* 37. <https://doi.org/10.1029/2009GL041345>
- Zhang L-X, Zhou D-C, Fan J-W, Hu Z-M (2015) Comparison of four light use efficiency models for estimating terrestrial gross primary production. *Ecol Model* 300:30–39. <https://doi.org/10.1016/j.ecolmodel.2015.01.001>
- Zhang Y, Hu Q, Zou F (2021) Spatio-temporal changes of vegetation net primary productivity and its driving factors on the Qinghai-Tibetan Plateau from 2001 to 2017. *Remote Sens* 13:1566. <https://doi.org/10.3390/rs13081566>
- Zhao M, Heinsch FA, Nemani RR, Running SW (2005) Improvements of the MODIS terrestrial gross and net primary production global data set. *Remote Sens Environ* 95(2):164–176. <http://dx.doi.org/10.1016/j.rse.2004.12.011>
- Zhao F, Xu B, Yang X, Jin Y, Li J, Xia L, Chen S, Ma H (2005) Remote sensing estimates of grassland aboveground biomass based on MODIS net primary productivity (NPP): a case study in the Xilingol Grassland of Northern China. *Remote Sens* 6:5368–5386. <https://doi.org/10.3390/rs6065368>
- Zhu Z, Piao S, Myneni RB, Huang M, Zeng Z, Canadell JG, Ciais P, Sitch S, Friedlingstein P, Arneeth A, Cao C, Cheng L, Kato E, Koven C, Li Y, Lian X, Liu Y, Liu R, Mao J, Pan Y, Peng S, Peuelas J, Poulter B, Pugh TAM, Stocker BD, Viovy N, Wang X, Wang Y, Xiao Z, Yang H, Zaehle S, Zeng N (2016) Greening of the Earth and its drivers. *Nat Clim Chang* 6(8):791–795. <https://doi.org/10.1038/nclimate3004>

Open Access This chapter is licensed under the terms of the Creative Commons Attribution 4.0 International License (<http://creativecommons.org/licenses/by/4.0/>), which permits use, sharing, adaptation, distribution and reproduction in any medium or format, as long as you give appropriate credit to the original author(s) and the source, provide a link to the Creative Commons license and indicate if changes were made.

The images or other third party material in this chapter are included in the chapter's Creative Commons license, unless indicated otherwise in a credit line to the material. If material is not included in the chapter's Creative Commons license and your intended use is not permitted by statutory regulation or exceeds the permitted use, you will need to obtain permission directly from the copyright holder.

